

# Tribological Properties and Acoustic Emissions of Some Thermoplastics Sliding Against SAE52100

**Habib S. Benabdallah**

Department of Mechanical Engineering,  
Royal Military College of Canada,  
PO Box 17000, Stn Forces,  
Kingston, Ontario, K7K 7B4, Canada  
e-mail: benabdallah-h@rmc.ca

*Measurements were made of the dynamic friction; wear volume and acoustic signal (AE) of several thermoplastics rubbing against smooth SAE-52100 steel. Polyoxymethylene, polyamide, poly(amide-imide), polypropylene, Poly(vinyl chloride), polytetrafluoroethylene, and polyethylene, were investigated using pin-on-disk configuration. Sliding speeds ranged from 0.05 to 0.45 m/s, and normal loads from 40 to 160 N (2–8 MPa) for sliding distances varying from 4 to 20 km. Orthogonal experimental design and analysis method was used to develop wear equations expressing wear volume as function of the operating parameters. Consistent relations were also found between the integrated AE signal over time and the wear volume as well as the friction work. [DOI: 10.1115/1.2000264]*

## Introduction

Many studies have so far been carried out to investigate the friction and wear behavior of different plastic materials when in dynamic contact with themselves or with metallic surface especially hard steel [1–3]. Various experimental conditions have been considered including the effect of the testing environment (dry, humid, lubricated with water or conventional lubricants also with additives). The majority of experimental setups used were in the form of pin-on-disk arrangements equipped in some cases with features that allow the removal of wear debris from the contact zone during sliding. Despite considerable effort some conflicting and sometimes unexpected results were found which did not contribute to finding useful correlations between tribological properties (friction and wear) and the operating conditions. The other major factor that complicates this task even more is the wide scatter that is often observed in the wear rate of plastic materials. Additionally, the wear rate variation could experience discontinuities when a certain threshold value of rubbing conditions is reached, thought to be associated to surface thermal effects. The performance of polymeric bearings is characterized not only by the level of friction but also wear generated under operating conditions appropriate for engineering applications. The challenge resides in the effort of developing models that could properly predict the wear of these materials, to be used during the design phase. Meng and Ludema [4] have extensively analyzed wear models and equations in the literature and recommended to rather translate the microscopic observations of the wearing process into macroscopic models. On the other hand, Zhang [5] has reviewed the progress in the understanding of polymer tribology. As a general guideline, Czichos et al. [6] have reported in an overview paper that materials suitable for dry tribological applications should yield a wear rate lower than  $10^{-6}$  mm<sup>3</sup>/N/m, a coefficient of friction lower than 0.2 both being independent of mild changes of the operating conditions.

When a polymeric material is rubbed against metal surface, adhesion, abrasion, and fatigue are the most recognized modes of wear that could occur. It is now accepted that when the metallic surface is smooth and hard, abrasion is negligible. A surface roughness of about 0.05 μm is often cited to be the threshold

above which abrasion mechanism becomes significant. The results of the weight loss due to wear of polymer based composite caused by sliding against smooth metallic surface were found by Rhee [7] to be satisfactorily described by the equation

$$\Delta m = CL^a V^b t^c \quad (1)$$

where  $\Delta m$  is the weight loss,  $C$  is the wear factor,  $L$  is the load,  $V$  is the relative speed, and  $t$  is the sliding time. The remaining parameters are constants for a given system. At the same time the author concluded that the wear factor  $C$  was practically constant for a given system.

Kar and Bahadur [8] performed a refinement of Eq. (1). It consisted of the incorporation of pertinent mechanical and thermal properties of the worn material yielding the following form:

$$w = kP^x V^{y-z} t^y \gamma^{3-y-z} E^{-3-x+y} \left(\frac{C_p}{K}\right)^z \quad (2)$$

Equation (2) relates the wear volume  $w$  to the experimental parameters, the load being expressed by the contact pressure  $P$  in this case. Apart from the constants  $k$ ,  $x$ ,  $y$ , and  $z$  that should be determined, the equation includes the surface energy  $\gamma$ , the modulus of elasticity  $E$ , the specific heat  $C_p$ , and thermal conductivity  $K$ . Expanding on this finding and based on a dimensional analysis, Viswanath and Bellow [9] have developed the following relationships that include the effect of the counterface roughness  $\alpha$ :

$$w = k_w L V t \alpha \gamma^{-1} \quad (3)$$

$$w = k_w L^p V^q t^r \alpha^s E^{-3+p+r+s} \gamma^{3-2p-q-s} (C_p/K)^{r-q} \quad (4)$$

However, their experimental results obtained using different plastics revealed in some cases unexpected high sensitivity of  $k_w$  with the operating parameters. More recently, Liu et al. [10] have been successful in describing the wear of two polymers in virgin state as well as blended together, using regression equations based on an orthogonal experimental and analysis method. Finally, Ravikiran [11] has also reported the large scatter in wear rate and showed that the ways of qualifying it could also be the cause. He then proposed a new nondimensional factor called wear index WI that incorporates the volume lost per unit sliding distance, the contact area, an aspect ratio of the dimensions of both triboelement along the friction path, as well as a factor that expresses the effectiveness of the layer (third body) formed on the contacting surfaces.

Contributed by the Tribology Division of ASME for publication in the JOURNAL OF TRIBOLOGY. Manuscript received February 14, 2003; final manuscript received November 12, 2004. Review conducted by M. D. Bryant.

It is clear that wear predictions with reasonable accuracy are important for designers of systems in which machine elements are subjected to dynamic contact. Also real time monitoring of wear itself could be cumbersome and complicated. Acoustic emissions (AE) have started to be used in early 70s to analyse vibration spectra during sliding friction of solids. Later on, researchers have shown the possibility of applying this technique to study the tribological behaviour of interfaces in relative motion. Various relationships have been so far proposed between different information of AE signal such as number of pulses per unit time, the frequency spectrum, amplitude (voltage), or energy of the signal and tribological properties. Different systems and triboelements have been considered under dry and lubricated environment [12–21]. The aim of this study was to develop wear equations for a wide range of thermoplastics that are potentially used as bearings in engineering applications. Another objective was to investigate whether the tribological properties of these materials could be linked to any information from AE signals in order to be able to predict wear and friction from on-line monitoring of AE.

### Experimental Procedure, Samples Preparation, and Materials

A designed pin-on-flat disk apparatus was used, powered by a 1 kW brushless motor that provided the rotating movement and torque to the disk through a flexible coupling thus preventing vibrations from being transmitted to the tribosystem. Rotating speeds were obtained with accuracy equivalent to  $\pm 0.1$  rpm. The sample (pin) holder was attached to a very rigid arm linked to the rig support by means of a horizontal pivot. The later was mounted on precision bearings, whose axis lies in the interfacial plane of initial contact between the pin and the disk and thus eliminating any moment that would otherwise be created by the friction force in dynamic state. The arm was balanced by a counterweight. Care was taken in order to ensure that the arm was perfectly horizontal at the beginning of each test. A force sensor equipped with silicon strain gauges was used to measure the friction force with a resolution of at least 0.05 N. Dead weight system was utilized to apply the normal load. The AE signal arising from the interaction of the surfaces in dynamic contact was detected by means of an acoustic emission transducer with a resonant frequency of 750 kHz acoustically coupled to the sample (pin) holder with silicon grease. The signal from the transducer was fed into a preamplifier (60 dB gain with a frequency range of 300–1000 kHz) and then channelled to a root-mean-square (rms) meter that in turn outputs the signal in the form of a voltage. The signals from both sensors were fed into a computer through a 12 bits data acquisition board.

Generally, AE signals fall into two categories: transient pulses (burst emissions) and pseudocontinuous emissions. The most common measurements used for burst emissions is what is known as ringdown counts which consists of counting the number of times the amplified AE signal crosses a preset trigger level voltage. The present study considered the pseudocontinuous emissions type, without imposing any threshold level on the measurement of this signal.

The tribometer was enclosed during testing in a Plexiglas box and care was taken to maintain the relative humidity of the environment at  $50\% \pm 5\%$  and the temperature at  $22 \text{ }^\circ\text{C} \pm 2 \text{ }^\circ\text{C}$ .

The disks were made of in-house machined SAE 52100 steel then heat treated to obtain very high hardness. Seven different thermoplastics in the form of pins cut from commercially available extruded rods were selected for this study. They are listed in Table 1, which includes pertinent properties taken from data supplied by the manufacturers. The technical specifications of both triboelements are listed in Table 2. Before testing all samples were placed into a beaker containing a 1 to 1 mixture of isooctane and isopropyl alcohol then ultrasonically cleaned for 15 min. After they were rinsed with acetone and dried, they were stored in desiccators. Special care was taken in order to ensure that the tribo-

**Table 1 Characteristics and properties of tested plastics**

Material and Grade	Designation	Tensile Modulus E (MPa)	Tensile Strength @ Break (MPa)	Thermal conductivity K (cal/s/°C/m <sup>2</sup> )	Specific heat Cp (cal/°C/m)	Surface energy $\gamma$ (J/m <sup>2</sup> )	Density (g/cm <sup>3</sup> )
Polyoxymethylene Delrin 500P	POM	3,250	68	$7.94 \times 10^{-4}$	0.35	0.0312	1.42
Polyamide Zytel 101 L C010	PA 66	2,700	78	$5.795 \times 10^{-4}$	0.42	0.035	1.14
Poly(amide-imide) Torlon-4203 L	Torlon	4,500	102	$6.2 \times 10^{-4}$	0.42	0.0343	1.412
Polypropylene Pro-fax 6323	PP	1,550	35	$5.99 \times 10^{-4}$	0.23	0.023	0.9
Polytetrafluoroethylene Teflon	PTFE	550	12	$5.86 \times 10^{-4}$	0.25	0.018	2.21
Polyethylene high density HD 9012	HDPE	1,100	28	$5.2 \times 10^{-4}$	0.55	0.0285	0.952
Poly(vinyl chloride) PVC-CAW	PVC	2,500	58	$2.8 \times 10^{-4}$	0.24	0.0347	1.42

surfaces were not contaminated before mounted onto the testing apparatus. A new set of materials was used at the beginning of each testing period.

After testing, the wear surface of the pin was carefully cleaned with a soft brush from loose debris and the mass loss was evaluated using a balance with an accuracy of  $\pm 0.001$  mg. The density reported in Table 1 was then used to derive the wear volume.

The experimental results were obtained after a reasonable number of trials carried out at repeated testing conditions and the data subsequently reported are average values. The number of tests was increased if repeatability was not satisfactory.

### Results and Discussion

**Wear.** It is well known that although wear is a property of the material, it strongly depends on the operating conditions. Most developed wear equations, among them those reported earlier (Eqs. (1)–(4)), contain proportionality constants such as the wear rate. Yet, as it will be shown below in the case of the wear rate, these constants can be significantly influenced by the operating parameters. The regression techniques are alternative ways of modeling and present the advantage of better relating the importance of each operating factor on the wear. The orthogonal analysis is a statistical method, which could be readily applied to find the parameters of this correlation that relates the studied parameters to the wear. This study dealt with the examination of the effects of the sliding distance  $s$ , apparent contact pressure  $P$ , and sliding velocity  $V$  on the wear volume. Based on this method, the test arrangement shown in Table 3 was developed. The levels of each operating condition characterizing each trial are listed as well as the resulting wear expressed in mass loss, for each polymer. Clearly, the test duration for each trial, which ranged from 2.5 h to 4.5 days, can be readily derived from the assessed param-

**Table 2 Experimental specifications of the triboelements**

Sample	Characteristics
Pin Plastic	Diameter 5 mm, tolerance $\pm 20 \text{ } \mu\text{m}$
	Contacting surface roughness: $R_a = 0.08 \text{ } \mu\text{m}$
	Length: 25 mm
Disc SAE 52100	External diameter: 50 mm
	Centred hole for holding purpose: 25 mm of diameter
	Thickness: 8.5 mm
	Contacting surface polished according to Buehler Dialog Method #10.01
	Maximum surface roughness: $R_a = 0.05 \text{ } \mu\text{m}$
	Hardness: HRC 63 to HRC 65

**Table 3 Array of the experimental parameters and resulting wear**

Trial #	s (km)	P (MPa)	V (m/s)	Wear expressed in mass loss (mg)						
				POM	PA66	Torlon	PP	PTFE	HDPE	PVC
1	4	8	0.05	0.298	0.239	0.234	0.198	446.420	0.286	0.142
2	4	6.5	0.15	0.341	0.228	0.264	0.157	351.390	0.226	0.213
3	4	5	0.25	0.270	0.160	0.193	0.198	221.000	0.286	0.426
4	4	3.5	0.35	0.114	0.125	0.081	0.078	154.700	0.112	0.167
5	4	2	0.45	0.071	0.069	0.071	0.054	83.980	0.571	0.071
6	8	8	0.15	0.852	0.570	0.407	0.794	811.070	1.142	0.994
7	8	6.5	0.25	0.682	0.473	0.488	0.582	634.270	0.837	0.710
8	8	5	0.35	0.554	0.384	0.396	0.609	442.000	0.877	0.426
9	8	3.5	0.45	0.312	0.217	0.224	0.450	243.100	1.142	0.284
10	8	2	0.05	0.156	0.167	0.173	0.090	134.810	1.093	0.142
11	12	8	0.25	1.136	0.886	0.915	1.669	1180.140	2.401	1.704
12	12	6.5	0.35	1.079	0.739	0.762	1.476	985.660	2.124	1.562
13	12	5	0.45	0.895	0.575	0.593	1.080	654.160	2.018	1.463
14	12	3.5	0.05	0.341	0.236	0.244	0.333	442.000	0.479	0.284
15	12	2	0.15	0.241	0.205	0.268	0.257	262.990	0.370	0.142
16	16	8	0.35	1.562	1.182	1.220	2.070	1569.100	3.332	2.982
17	16	6.5	0.45	1.448	1.044	1.078	1.530	1211.080	3.142	2.414
18	16	5	0.05	1.108	0.768	0.793	0.720	881.790	0.394	0.587
19	16	3.5	0.15	0.710	0.492	0.508	0.306	581.230	0.186	0.277
20	16	2	0.25	0.469	0.353	0.396	0.252	198.900	0.577	0.227
21	20	8	0.45	1.988	1.482	1.553	3.150	1940.380	5.085	4.047
22	20	6.5	0.05	1.562	1.083	1.118	1.890	1613.300	1.525	1.278
23	20	5	0.15	0.994	0.775	0.712	1.080	1027.650	1.000	0.852
24	20	3.5	0.25	0.852	0.616	0.610	0.747	735.930	1.075	0.710
25	20	2	0.35	0.625	0.479	0.447	0.595	320.450	0.857	0.497

eters  $s$  and  $V$ .

The specific wear rate  $K_0$  defined as the wear volume per unit load and unit sliding distance is mostly used for wear qualification and often quoted as an indicator of the performance of the material. An example of the wear results expressed by  $K_0$  obtained according to the experimental parameters arranged as shown in Table 3, is depicted against the parameter  $PV$  in Fig. 1 for all experimented sliding distances. The figure indicates in general a large scatter with the operating condition and although an approximate average value could be derived for some materials, a continuous increase is apparent for others. These results are summarized in Table 4 as the average value of  $K_0$  together with the standard deviation  $\sigma$  normalized with respect to that average and listed in percentage. Power equation approximated through curve fitting is proposed when the trend shows an increase. The data in Table 4 could be used for material selection and comparison process but clearly the design of bearings for critical applications requires equations that would predict more accurately the amount of wear and its progression with the time.

Coming back to the wear modeling, the determination of the regression constants of the equation relating the wear volume to the experimental parameters according to the orthogonal analysis

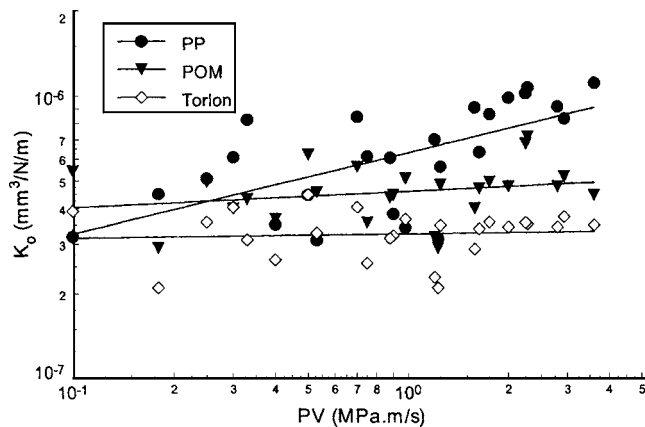


**Fig. 1 Specific wear rate as a function of  $PV$  for PP, POM, and Torlon**

**Table 4 Average values or trends of  $K_0$  and normalized standard deviation**

	$K_0$ (mm <sup>3</sup> /N/m)	$\sigma$ (%)
POM	$4.68 \times 10^{-7}$	22.6
PA 66	$4.02 \times 10^{-7}$	13.7
Torlon	$3.31 \times 10^{-7}$	18.2
PP	$6.3 \times 10^{-7} PV^{0.287}$	39.5
PTFE	$2.54 \times 10^{-4}$	16
HDPE	$9.6 \times 10^{-7} PV^{0.226}$	76
PVC	$4.27 \times 10^{-7} PV^{0.426}$	51

requires the construction of a matrix, which contains the investigated parameters in a normalized form. The aim of this operation is mainly to facilitate the manipulation of the data necessary for the determination of the correlation constants. The preliminary investigation has permitted us to conclude that the second order form expressed without any interaction between the parameters was sufficient to adequately correlate the wear volume to the testing parameters. According to code, the first and the second order normalized forms of each investigated parameter, called  $OC'$  and  $OC''$ , are obtained using Eqs. (5) and (6). Note that Eq. (6) contains two constants  $c_1$  and  $c_2$  whose values should be chosen in order to yield normalized values varying within the same range for all considered operating conditions, respectively. By choosing  $c_1=1$  and  $c_2=2$  all were found to vary between  $-2$  and  $+2$  in the case of this study

$$OC'_i = \frac{OC_i - \overline{OC}}{\Delta(OC)} \quad (5)$$

$$OC''_i = c_1 \left[ \left( \frac{OC_i - \overline{OC}}{\Delta(OC)} \right)^2 - c_2 \right] \quad (6)$$

The value of each operating condition is labeled  $OC$ , varies within a certain range characterized by an average value  $\overline{OC}$  ( $\overline{OC} = 12$  km for  $s$ , 5 MPa for  $P$  and 0.25 m/s for  $V$ ) and a constant increment  $\Delta(OC)$ , ( $\Delta s=4$  km,  $\Delta P=1.5$  MPa,  $\Delta V=0.1$  m/s). The subscript  $i$  refers to the trial number. The results of this normalizing process constitute the entries for each column of Table 5. It is to note that the matrix contains an extra column filled with entries equal to 1 that will serve to determine the correlation independent constant.

The calculation of the regression coefficients forming the last row of the matrix and labelled  $b_k$  requires the preliminary evaluation of parameters  $B_k$  and  $D_k$  according to Eqs. (7) and (8); knowing the wear volume  $w_i$  (mm<sup>3</sup>). The components of array  $B_k$  are obtained by summing the squared values of entries in the corresponding columns. These entries are in fact the normalized values of the assessed operating conditions. Subscript  $k$  varies between 1 and a value equivalent to the product of the number of the considered operating conditions and the chosen order of the regression. Note that  $B_1$  is associated with the independent constant and that the maximum value of  $k$  in this case is 6. The measured wear volume is involved in the determination of array  $D_k$

$$B_k = \sum_{i=1}^{i=25} (OC'_i)^2 \text{ or } \sum_{i=1}^{i=25} (OC''_i)^2 \quad (7)$$

$$D_k = \sum_{i=1}^{i=25} (OC'_i)(w_i) \text{ or } \sum_{i=1}^{i=25} (OC''_i)(w_i) \quad (8)$$

The above outlined reasoning applies also to the independent constant. Finally, the inverse ratio of these two quantities  $B_k$  and  $D_k$  gives the regression coefficients represented by array  $b_k$ . Table 5

**Table 5 Arrangement of the experimental conditions and results of the orthogonal analysis**

Trial # (i)	s (km)	P (MPa)	V (m/s)	Const.	OC <sub>i</sub> , OC <sub>i</sub> '							
					OC <sub>1</sub> '		OC <sub>2</sub> '		OC <sub>3</sub> '		OC <sub>4</sub> '	
					For s	For P	For V	For V	For V	For V	For V	For V
1	4	8	0.05	1	-2	2	2	2	-2	2	2	
2	4	6.5	0.15	1	-2	2	1	-1	-1	-1	-1	
3	4	5	0.25	1	-2	2	0	-2	0	-2	-2	
4	4	3.5	0.35	1	-2	2	-1	-1	1	-1	-1	
5	4	2	0.45	1	-2	2	-2	2	2	2	2	
6	8	8	0.15	1	-1	-1	2	2	-1	-1	-1	
7	8	6.5	0.25	1	-1	-1	1	-1	0	-2	-2	
8	8	5	0.35	1	-1	-1	0	-2	1	-1	-1	
9	8	3.5	0.45	1	-1	-1	-1	-1	2	2	2	
10	8	2	0.05	1	-1	-1	-2	2	-2	2	2	
11	12	8	0.25	1	0	-2	2	2	0	-2	-2	
12	12	6.5	0.35	1	0	-2	1	-1	1	-1	-1	
13	12	5	0.45	1	0	-2	0	-2	2	2	2	
14	12	3.5	0.05	1	0	-2	-1	-1	-2	2	2	
15	12	2	0.15	1	0	-2	-2	2	-1	-1	-1	
16	16	8	0.35	1	1	-1	2	2	1	-1	-1	
17	16	6.5	0.45	1	1	-1	1	-1	2	2	2	
18	16	5	0.05	1	1	-1	0	-2	-2	2	2	
19	16	3.5	0.15	1	1	-1	-1	-1	-1	-1	-1	
20	16	2	0.25	1	1	-1	-2	2	0	-2	-2	
21	20	8	0.45	1	2	2	2	2	2	2	2	
22	20	6.5	0.05	1	2	2	1	-1	-2	2	2	
23	20	5	0.15	1	2	2	0	-2	-1	-1	-1	
24	20	3.5	0.25	1	2	2	-1	-1	0	-2	-2	
25	20	2	0.35	1	2	2	-2	2	1	-1	-1	
				<i>B<sub>k</sub></i>	25	50	70	50	70	50	70	70
				<i>D<sub>k</sub></i>	13.888	9.09	-1.9	8.1	-0.6	3.22	1.76	
				<i>b<sub>k</sub></i>	0.556	0.182	-0.027	0.162	-0.0083	0.06	0.025	

shows the results for POM.

An example of the calculation of OC' and OC'' for *s* corresponding to trial No. 1 chosen for clarification follows; note that *c*<sub>1</sub>=1 and *c*<sub>2</sub>=2:

$$OC'_i = \frac{OC_i - \overline{OC}}{\Delta(OC)} = \frac{4 - 12}{4} = -2$$

$$OC''_i = c_1 \left[ \left( \frac{OC_i - \overline{OC}}{\Delta(OC)} \right)^2 - c_2 \right] = 1 \left[ \left( \frac{4 - 12}{4} \right)^2 - 2 \right] = 2$$

The results of Table 5 yielded Eq. (9) that expresses the relationship between the wear volume *w* and the investigated operating conditions

$$w = 0.556 + 0.182 \left( \frac{s - 12}{4} \right) - 0.027 \left[ \left( \frac{s - 12}{4} \right)^2 - 2 \right] + 0.162 \left( \frac{P - 5}{1.5} \right) - 0.008 \left[ \left( \frac{P - 5}{1.5} \right)^2 - 2 \right] + \dots - 0.064 \left( \frac{V - 0.25}{0.1} \right) + 0.025 \left[ \left( \frac{V - 0.25}{0.1} \right)^2 - 2 \right] \quad (9)$$

This equation contains the independent constant as well as all regression coefficients taken from Table 5 (see last row labeled *b<sub>k</sub>*) that were applied, respectively, to the first and second order normalized forms of the investigated parameters (Eqs. (5) and (6)).

By grouping the compatible terms of Eq. (9), the regression equation relating the wear volume to the experimental parameters is written in the following general form:

$$w = k_0 + k_{11}s + k_{12}s^2 + k_{21}P + k_{22}P^2 + k_{31}V + k_{32}V^2 \quad (10)$$

The corresponding values of the constants for Eq. (10) are summarized in Table 6 for all tested materials. These constants have no physical meaning and therefore were treated as dimensionless quantities. But, it is important to mention that their listed values apply only when the operating parameters *s*, *P*, and *V* are expressed in km, MPa, and m/s respectively; yielding a wear volume in mm<sup>3</sup>. In addition, it is clear that the proposed equation of wear

**Table 6 Values of the constants for Eq. (10)**

	<i>k</i> <sub>0</sub>	<i>k</i> <sub>11</sub>	<i>k</i> <sub>12</sub>	<i>k</i> <sub>21</sub>	<i>k</i> <sub>22</sub>	<i>k</i> <sub>31</sub>	<i>k</i> <sub>32</sub>
POM	-0.851	0.086	-0.0017	0.145	-0.004	-0.614	2.517
PA 66	-0.461	0.049	-0.0003	0.056	0.004	-0.582	2.014
Torlon	-0.396	0.044	-0.0004	0.048	0.003	-0.579	1.911
PP	-1.159	0.106	-0.0007	0.016	0.024	-1.865	7.418
PTFE	-293.8	24.42	0.0134	61.50	1.410	-772.1	1845.7
HDPE	-0.843	0.221	-0.0051	-0.448	0.076	-3.815	16.344
PVC	-0.963	0.097	-0.0016	-0.083	0.029	-0.805	5.792

prediction reflects principally the phase of equilibrium wear.

According to statistics analysis, the degree of control *R*, at which a certain parameter affects the wear can be determined as follows:

$$R = \max\{\bar{w}_n\} - \min\{\bar{w}_n\} \quad (11)$$

in which  $\bar{w}_n$  is the average wear generated by the effect of the remaining parameters when the considered one remains constant. Equivalent equation is applicable for the evaluation of the effect of the other testing parameters. The results pertaining to the present study are summarized in Table 7, level 1 (*R*=1) denoting the testing parameter that controls the most the wear volume.

The data of Table 7 reveal that the range of speed investigated had lesser effect on the wear of all materials with the exception of HDPE. It is recognized that the sliding speed contributes the most to the increase of the interface temperature in dry conditions, which in turn affects the wear mechanism. HDPE having the lowest softening temperature explains the higher sensitivity of its wear to the sliding speed. On the other hand, the contact pressure was found to be the dominant factor on the wear of PTFE. This is a soft material with low surface hardness therefore more susceptible to indentation by the asperities of the metallic counterface that cause microcutting accentuated by the relatively high normal load. It is believed that these conditions tend to hinder the beneficial effect of film formation and transfer for which PTFE is recognized. For all remaining plastics, mostly the sliding distance influences the wear volume. This finding reveals that severe wear is generated when POM, PA 66, Torlon, PP, and PVC are subjected to extreme sliding distance. Therefore, one or the combination of more of the following phenomena may take place under this condition: surface fatigue; upset of transfer film; creation of abrasive environment induced by metallic debris from the counterface. All these mechanisms are known to produce severe wear. Conversely, due to their good mechanical properties especially the tensile strength (see Table 1), wear of these materials is influenced to a lesser degree by the contact pressure followed by the sliding speed.

Figure 2 was constructed to evaluate the developed relationship between the wear volume and the load. It was obtained by plotting the experimental results depicted by the symbols together with the

**Table 7 Degree of control of each testing parameter on the wear volume**

	<i>s</i>	<i>P</i>	<i>V</i>
POM	1	2	3
PA 66	1	2	3
Torlon	1	2	3
PP	1	2	3
PTFE	2	1	3
HDPE	3	2	1
PVC	1	2	3

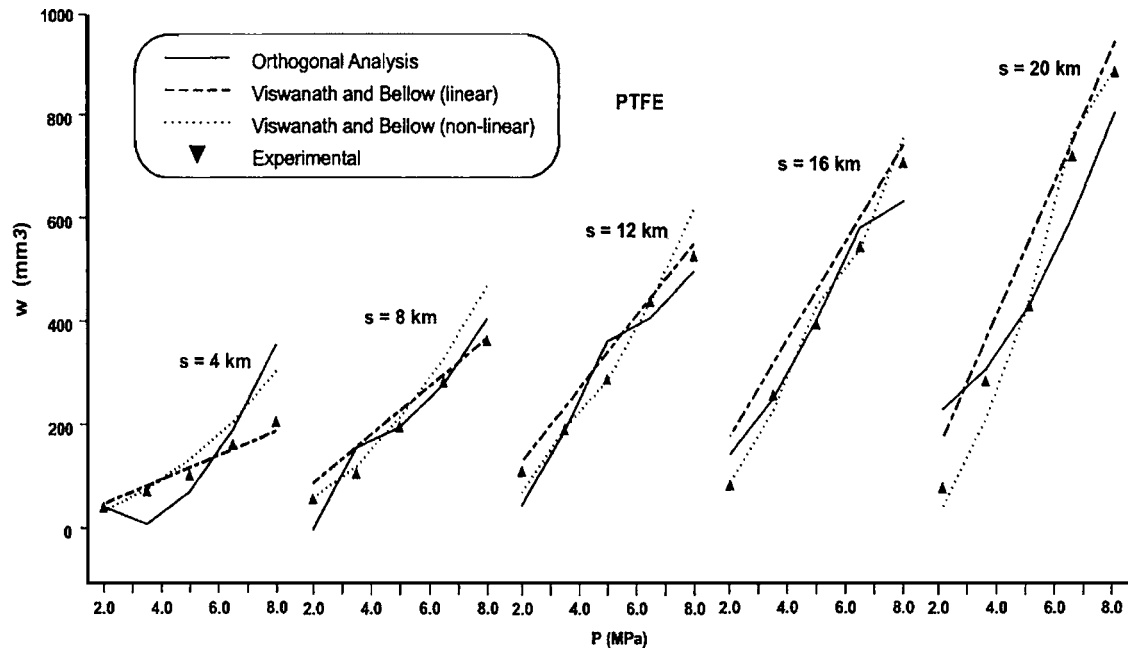


Fig. 2 Experimental and predicted wear volume as function of  $P$  for PTFE

predicted trend represented by lines. The case of PTFE was taken as an example. The plots generated using the linear and nonlinear equations [9] were also included for the purpose of comparison.

These data illustrate that although some scatter is apparent the trend is reasonably well predicted by all models. A closer look reveals that the precision of each model depends on the level of wear. For instance, the linear equation seems to predict better low levels of wear. The intermediate levels are better represented by orthogonal analysis. On the other hand, the nonlinear model is more adequate for predicting higher levels of wear. But this observation did not apply to all tested plastics. In fact we were unable to make the nonlinear model converge toward a solution that fits reasonably well the experimental data for the case of POM, PA 66, and Torlon due to the very high sensitivity of the wear coefficient with the operating variables. It was noted that these three materials were characterized by low wear and high tensile modulus. Nevertheless, it was felt interesting to report below the non-linear equations that were developed for PP, PTFE, HDPE, and PVC, respectively,

$$w_{\text{mod}} = 1.021 \times 10^{-16} L^{1.631} V^{1.75} t^{1.01} \quad (12)$$

$$w_{\text{mod}} = 1.633 \times 10^{-16} L^{1.31} V^{2.4} t^{1.22} \quad (13)$$

$$w = 2.054 \times 10^{-13} L^{1.497} V^{0.695} t^{0.772} \quad (14)$$

$$w_{\text{mod}} = 1.977 \times 10^{-16} L^{2.041} V^{1.152} t^{0.679} \quad (15)$$

Finally, it was found that in all cases both the orthogonal analysis as well as the linear model yielded best fit of the experimental results. The derived wear coefficient  $k_w$  of the linear model (Eq. (3)) is presented for each material in Table 8. It worth repeating that Eq. (3) is dimensionally homogeneous in terms of the specified variables and therefore the proportionality constant  $k_w$  is dimensionless.

**Acoustic emissions.** Figure 3 shows typical AE rms voltages during the first 5000 s of testing at the conditions of trial No. 10 (see Table 3). These signals clearly show two apparent regions, one characterized by unsteady variations pertaining to the running-in period followed by a leveling off corresponding to equilibrium state of the wear rate and friction. Similar behavior has also been reported for the case of metallic specimens in rela-

tive sliding motion [19]. At the same time, each material is characterized by distinct form of AE signal. Knowing that these signals arise from the release of mechanical stress waves created by deformation of the material surface, different steady state levels should be observed for materials of different mechanical and morphological properties rubbing against the same counterface at the same operating conditions. The present results are in agreement

Table 8 Wear coefficients for the linear model

	$k_w$
POM	$2.92 \times 10^{-10}$
PA 66	$3.12 \times 10^{-10}$
Torlon	$2.27 \times 10^{-10}$
PP	$4.39 \times 10^{-10}$
PTFE	$1.08 \times 10^{-7}$
HDPE	$8.08 \times 10^{-10}$
PVC	$3.19 \times 10^{-10}$

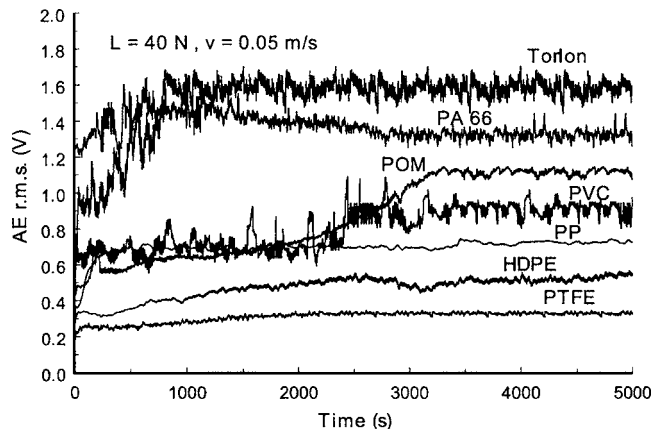


Fig. 3 Acoustic emission signals as function of time for all tested plastics

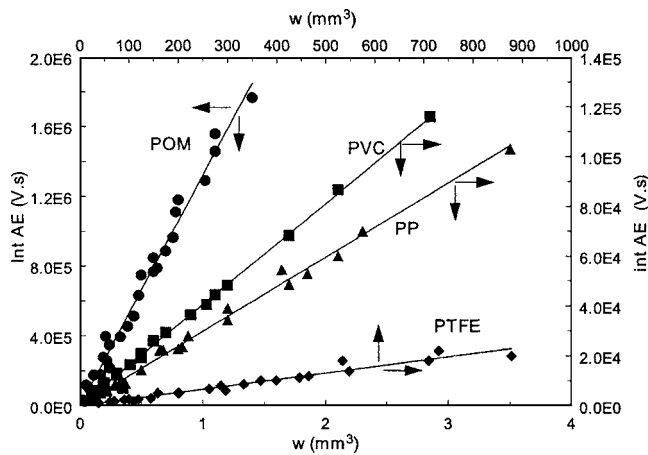


Fig. 4 Relationship between the integrated AE signal and the wear volume

with this analysis and further suggest that a direct relationship between the AE level under steady state and the tensile strength at break (see Table 1) may exist. Specifically, they indicate that higher is the strength of the material higher is the steady state AE signal. It is to note that the steady state value itself was observed to be a function of  $PV$  level. Moreover, the signals pertaining to the materials that are more susceptible to stick-slip phenomenon, such as PA66, PVC, and Torlon are characterized by higher fluctuations. This is due to the fact that microvibrations excited by the stick-slip at the interface can be an additional source of AE.

The relationship between wear and AE signal was investigated. Plots of the specific wear rate  $K_0$  against the integrated AE rms voltage over the sliding time, called int AE and which was obtained by a rectangular summing process, revealed a large scatter with random distribution. This is due to the observed high sensitivity of  $K_0$  with the operating parameters.

However, reasonable correlation between int AE and wear volume existed. Figure 4, which summarizes the results obtained under all experimented parameters for the case of three materials taken as example. It shows that int AE increases with the increase of the wear volume of the pin. In this study, this relationship can be modeled by linear dependence for all materials as follows:

$$\text{int AE} = \int \text{AE} dt = k_{\text{AE}} w \quad (16)$$

The values of the proportionality constant  $k_{\text{AE}}$  applicable to this study are reported in Table 9.

It is clear that the constant  $k_{\text{AE}}$  depends on the calibration of the AE signal. In practice, if different measuring system is used, few experiments should be conducted followed by a linear curve fitting of the results whose slope corresponds to the value of the constant.

Contrary to the present findings, power law expressions have been suggested in previous investigations to illustrate the depen-

Table 9 Values of the constant  $k_{\text{AE}}$

	$k_{\text{AE}} (\text{V.s/mm}^3)$
POM	$1.32 \times 10^6$
PA 66	$4.66 \times 10^4$
Torlon	$6.17 \times 10^4$
PP	$2.89 \times 10^4$
PTFE	26.15
HDPE	$3.04 \times 10^3$
PVC	$4.05 \times 10^4$

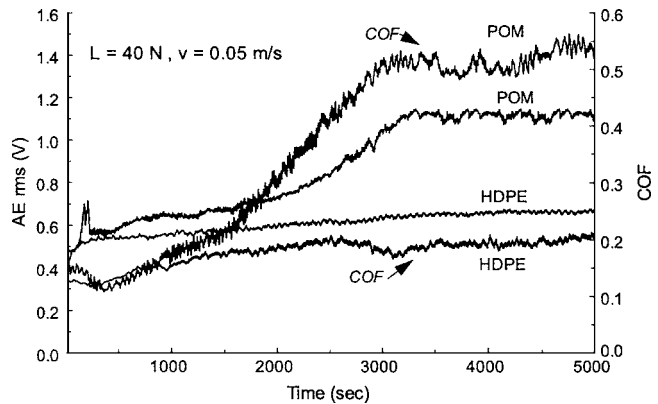


Fig. 5 Variation of COF and AE with the time for POM and HDPE

dence of AE rms voltage or count on wear rate or wear volume for different non-polymeric materials in dry rubbing contact [15,17,19] or lubricated with different types of lubricants [13]. Nevertheless, linear variation of the mass loss by wear with the total AE was arrived at Ref. [12] resulting from tests conducted on different polymers rubbing against high carbon steel under non-conformal contact geometry. The authors have based the interpretation of such relationship on the assumption that each particle separation in an isolated source of AE generation, both events being characterized by similar probability distribution. It is believed that the linear type is typical to plastic/steel friction when adhesion is prevalent. Plastic materials possess properties such as viscoelastic behavior, susceptibility to creep, and thermal effects that distinguish them from the other group.

Figure 5 depicts the simultaneous variations of the coefficient of friction (COF) and AE rms voltage during the first 5000 s of rubbing for the case of POM and HDPE taken as examples. The traces pertaining to COF were identified in the figure for both plastics. Comparable trend is displayed suggesting that some relationship may exist between these parameters. The spikes contained in the friction signal are generated by the adhesion phenomenon that induces deformation of the asperities. The initial peak of the AE signal is associated with an early removal of material taking place during the running-in process. But despite the compatible trend no correlation could be found between the two parameters when all testing conditions were considered. On the other hand, there are suggestions of the existence of close relationship between AE and friction work from sliding contact of pairs of materials. An attempt is made to investigate the possibility of identifying such for the case of the tribosystems considered in this study in which plastic materials are involved. The friction work  $F_w$  is defined by the following equation:

$$F_w = \int F_f ds \quad (17)$$

This represents the real time variation of the friction force  $F_f$ , integrated over the sliding distance. The data derived under the conditions of trial No. 10, that permitted to construct Fig. 6, show the existence of a reasonable correlation between int AE and  $F_w$  that was approximated by a linear relationship whose proportionality constant depends on the material. It is at this stage pertinent to mention the work of Lingard and Ng [22] who found a systematic relationship between cumulative AE count and frictional work, using disk on disk configuration (one fixed) to conduct dry friction experiments at a wide range of tribological conditions on six different metallic materials. Other authors [16] have concluded that the acoustic emission at the interface slider/disk was proportional to the work of friction per unit time (friction power). As pointed out earlier, the adhesion mechanism is predominant in this

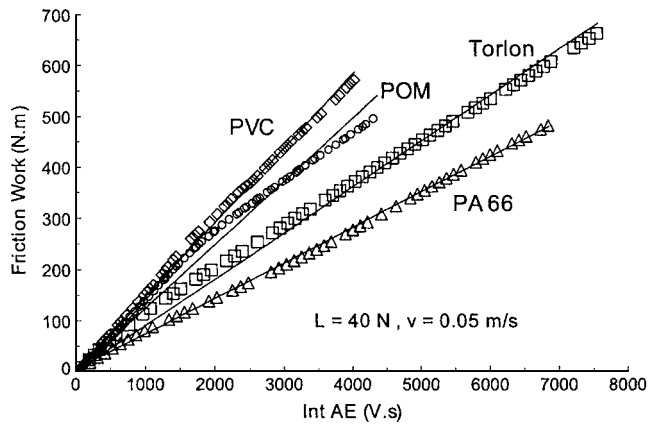


Fig. 6 Friction work as function of the integrated AE signal

study. Therefore, one can assume that an important part of the stress waves is generated by the shear strain energy from the material surface. This could explain the good correlation between  $F_w$  and AE. On the other hand, AE is related to the material removal power in an abrasive process [14].

It was shown that it is promising to establish useful relationships that could be used for predicting the tribological properties (friction and wear) of similar tribosystems, if on-line monitoring of AE signal is possible.

## Conclusion

A designed pin-on-disk tribometer was used to conduct the friction and wear testing as well as acoustic emissions measurements. Seven different thermoplastics were rubbed against SAE 52100 polished surface, under a wide range of operating conditions. Based on the obtained results, the following conclusions can be drawn.

The wear volume can be reasonably well correlated to the operating parameters (sliding distance, speed, and contact pressure) by a second order equation derived from the orthogonal experimental and analysis method.

A statistical analysis of the data revealed the highest degree of control of the sliding distance on the wear volume for all plastics with the exception of PTFE and HDPE. Due to its softness, the pressure mostly influences the wear behaviour of PTFE. The wear of HDPE is more influenced by the sliding speed owing to its low softening temperature.

Linear relationships exist between the wear volume under steady state and the integrated AE rms voltage for all tested plastics.

Although no direct relationship was found between the friction and AE signal, the same trend characterizes their variation with the time and it is possible to distinguish between the running-in and steady state regimes from AE signal.

The friction work is proportional to the integrated AE rms voltage.

The found relationships are important for the prediction of tribological behavior using on-line monitoring of AE signal.

## Acknowledgments

The author acknowledges the financial aid from NSERC Canada.

## References

- [1] Santner, E., and Czichos, H., 1989, "Tribology of Polymers," *Tribol. Int.* **22**, pp. 103–109.
- [2] Klapperich, C., Komvopoulos, K., and Pruitt, L., 1999, "Tribological Properties and Microstructure Evolution of Ultra-High Molecular Weight Polyethylene," *ASME J. Tribol.*, **121**, pp. 394–402.
- [3] Lee, J. H., Xu, G. H., and Liang, H., 2001, "Experimental and Numerical Analysis of Friction and Wear Behavior of Polycarbonate," *Wear*, **251**, pp. 1541–1556.
- [4] Meng, H. C., and Ludema, K. C., 1995, "Wear Models and Predictive Equations: Their Form and Content," *Wear*, **181–183**, pp. 443–457.
- [5] Zhang, S. W., 1998, "State-of-the-Art of Polymer Tribology," *Tribol. Int.*, **31**, pp. 49–60.
- [6] Czichos, H., Klaffke, D., Santner, E., and Woydt, M., 1995, "Advances in Tribology: The Materials Point of View," *Wear*, **190**, pp. 155–161.
- [7] Rhee, S. K., 1970, "Wear Equation for Polymers Sliding Against Metal Surfaces," *Wear*, **16**, pp. 431–445.
- [8] Kar, M. K., and Bahadur, S., 1974, "The Wear Equation for Unfilled and Filled Polyoxymethylene," *Wear*, **30**, pp. 337–348.
- [9] Viswanath, N., and Bellow, D. G., 1995, "Development of an Equation for the Wear of Polymers," *Wear*, **181–183**, pp. 42–49.
- [10] Liu, C. Z., Ren, L. Q., Tong, J., Green, S. M., and Arnell, R. D., 2001, "Statistical Wear Analysis of PA-6/UHMWPE Alloy, UHMWPE and PA-6," *Wear*, **249**, pp. 31–36.
- [11] Ravikiran, A., 2000, "Wear Qualification," *ASME J. Tribol.*, **122**, pp. 650–656.
- [12] Belyi, V. A., Kholodilov, O. V., and Sviridyonok, A. I., 1981, "Acoustic Spectrometry as Used for the Evaluation of Tribological Systems," *Wear*, **69**, pp. 309–319.
- [13] Boness, R. J., and McBride, S. L., 1991, "Adhesive and Abrasive Wear Studies Using Acoustic Emission Techniques," *Wear*, **149**, pp. 41–53.
- [14] Matsuoka, K., Forrest, D., and Tse, M.-K., 1993, "On-Line Wear Monitoring Using Acoustic Emission," *Wear*, **162–164**, pp. 605–610.
- [15] Benabdallah, H. S., and Boness, R. J., 1999, "Tribological Behaviour and Acoustic Emissions of Alumina, Silicon Nitride and SAE52100 Under Dry Sliding," *J. Mater. Sci.*, **34**, pp. 4995–5004.
- [16] Khurshudov, A. G., and Talke, F. E., 1998, "A Study of Subambient Pressure Tri-Pad Sliders Using Acoustic Emission," *ASME J. Tribol.*, **120**, pp. 54–59.
- [17] Matsuoka, K., Taniguchi, K., and Nakakita, M., 2001, "In-Situ Wear Monitoring of Slider and Disk Using Acoustic Emission," *ASME J. Tribol.*, **123**, pp. 175–180.
- [18] Jiaa, C. L., and Dornfeld, D. A., 1990, "Experimental Studies of Sliding Friction and Wear Via Acoustic Emission Signal Analysis," *Wear*, **139**, pp. 403–424.
- [19] Lingard, C. W., Yu, C. W., and Yau, C. F., 1993, "Sliding Wear Studies Using Acoustic Emission," *Wear*, **162–164**, pp. 597–604.
- [20] Cho, C.-W., and Lee, Y.-Z., 2000, "Wear-Life Evaluation of CrN-Coated Steels Using Acoustic Emission Signals," *Surf. Coat. Technol.*, **127**, pp. 59–65.
- [21] Hisakado, T., and Warashina, T., 1998, "Relationship Between Friction and Wear Properties and Acoustic Emission Characteristics: Iron Pin on Hardened Bearing Steel Disk," *Wear*, **216**, pp. 1–7.
- [22] Lingard, S., and Ng, K. K., 1989, "An Investigation of Acoustic Emission in Sliding Friction and Wear of Metals," *Wear*, **130**, pp. 367–379.